Origin and elimination of spurious solutions of the eight-band k·p theory

W. Yang and Kai Chang*
NLSM, Institute of Semiconductors, Chinese Academy of Sciences, P.O. Box 912, Beijing 100083, China
(Received 21 July 2005; revised manuscript received 9 September 2005; published 28 December 2005)

The origin of spurious solutions in the eight-band envelope function model is examined and it is shown that spurious solutions arise from the additional spurious degeneracies caused by the unphysical bowing of the conduction bands calculated within the eight-band **k·p** model. We propose two approaches to eliminate these spurious solutions. Using the first approach, the wave vector cutoff method, we demonstrate the origin and elimination of spurious solutions in a transparent way without modifying the original Hamiltonian. Through the second approach, we introduce some freedom in modifying the Hamiltonian. The comparison between the results from the various modified Hamiltonians suggests that the wave vector cutoff method can give accurate enough description to the final results.

DOI: 10.1103/PhysRevB.72.233309 PACS number(s): 73.21.−b, 02.60.−x

The envelope function approximation has been widely used in the calculation of electronic states in semiconductor nanostructures. In the eight-band model for narrow-gap semiconductor structures, the coupling between the conduction and the valence bands is considered exactly, while the effect of remote bands is taken into account through second-order perturbation theory.[1,2] This perturbative nature of the eight-band model leads to the problem of spurious solutions.[3–14] Spurious evanescent solutions[3] are shown to be of no physical significance[4,5] and are harmless in the calculation. Spurious oscillatory states,[6,7] however, are troublesome because they mix and interact with real states, making it difficult to identify and remove them in numerical calculations. To get rid of these spurious solutions, various proposals have been given, including the modification of band parameters[7,8] and introducing additional terms into the Hamiltonian.[9]

In this paper, the problem of spurious oscillatory solutions is examined and it is found that they come from the additional spurious degeneracies caused by the unphysical bowing of the conduction bands for the constituent materials calculated from the eight-band model. We propose two approaches to exclude such spurious degeneracies and, consequently, to eliminate these spurious solutions: (i) The wave vector cutoff method, i.e., restricting the wave vector of the envelope function in the monotonic region of the bulk energy bands. (ii) Modifying the original Hamiltonian to produce monotonic bulk bands. Using the first approach, the spurious solutions can be identified and removed without modifying the original Hamiltonian. A simple finite plane-wave expansion method is used and the origin and elimination of spurious solutions are demonstrated in a transparent way. For the second approach, we extend the existing proposals[8,9] to introduce some freedom in modifying the original Hamiltonian. The resulting different modified Hamiltonians are compared and we find that the difference between the results is within several meV. It suggests that the wave vector cutoff method, which does not modify the original Hamiltonian, gives accurate enough description to the final results.

Considering the electronic states of a [001] $(In_{0.53}Ga_{0.47}As)_{10}(InP)_{10}$ superlattice, the band parameters can be found in Ref. 15. The bulk band structures of InGaAs obtained from the **k·p** model and the more accurate empirical pseudopotential method[16] are plotted in Fig. 1. It can be seen that both methods give nonmonotonic conduction bands. However, the conduction band from the **k·p** model bows unphysically across the forbidden gap into the valence band at large wave vector $|k_z| > k_c$, introducing additional spurious degeneracies for a given energy (e.g., the states at k_2 and k_3 are degenerate in energy, but k_3 is a spurious degeneracy point). It is these spurious degeneracies that causes the appearance of spurious oscillatory solutions (these fast oscillating spurious solutions can be recognized by plotting their envelope functions).

To demonstrate the origin and elimination of spurious solutions in a transparent way, we use the finite plane-wave expansion method.[10] We notice that Winkler and Rössler (Ref. 10) briefly mentioned that a wave vector cutoff $|\mathbf{k}| \ll 2\pi/a$ (a is the lattice constant) can be used to avoid spurious solutions. However, the applicability of this approach and the detailed choice of the maximum cutoff wave vector k_0 to ensure the successful elimination of spurious solutions

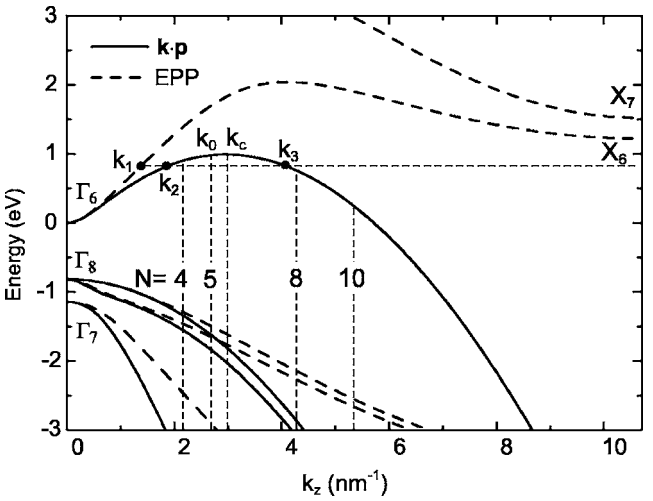

FIG. 1. Band structures of bulk InGaAs as a function of k_z for $\mathbf{k}_{\|}=0$. Solid and dashed lines are from the eight-band **k·p** model and the empirical pseudopotential method, respectively.

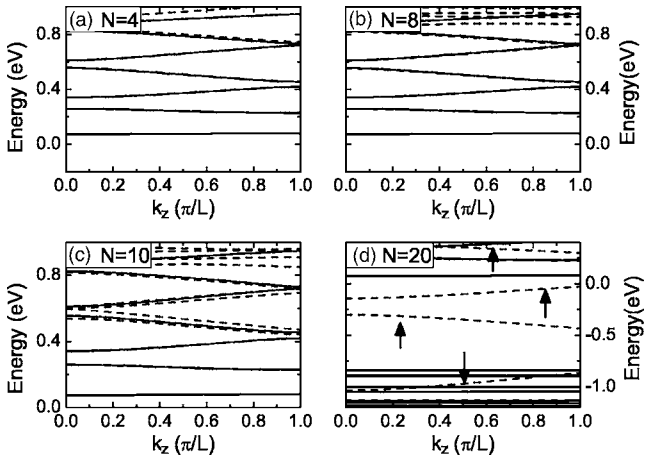

FIG. 2. Calculated subband structure (dashed lines) using different cutoff numbers N=(a) 4, (b) 8, (c) 10, and (d) 20. In all panels, the solid lines correspond to those calculated with N=5.

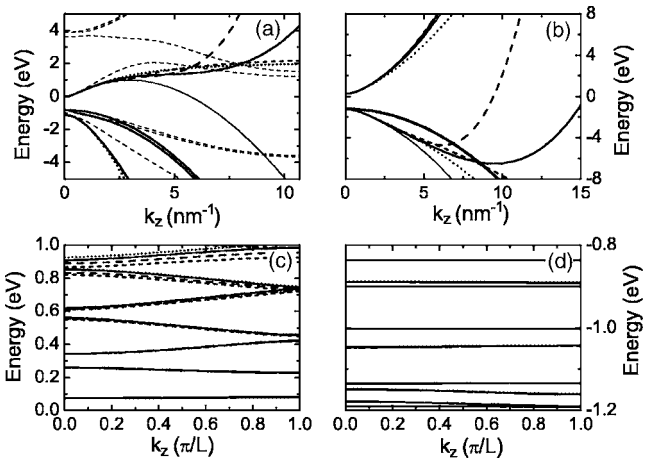

FIG. 3. Band structures of bulk (a) InGaAs and (b) InP as functions of k_z at $\mathbf{k}_\parallel=0$. Thin solid (thin dashed) lines are for the original eight-band $\mathbf{k}\cdot\mathbf{p}$ model (empirical pseudopotential method). (c) and (d) show the resulting superlattice subbands at $\mathbf{k}_\parallel=0$. In all panels, the solid, dashed, short dashed, and dotted lines are for the modified $\mathbf{k}\cdot\mathbf{p}$ models (i)–(iv), respectively. The cutoff number is N=10 for (ii) and N=15 for the others.

have not been demonstrated yet. In Fig. 2, we plot the subbands at $\mathbf{k}_\parallel=0$ calculated with different cutoff numbers N. Here $N=k_0L/(2\pi)$, where L is the period of the superlattice. It can be seen that no spurious solutions appear for N=4 or 5. For N=8 and 10, spurious solutions appear at energies above 0.8 and 0.4 eV, respectively, while for N=20, spurious solutions begin to enter the forbidden gap and the valence bands [indicated by the arrows in Fig. 2(d)]. This interesting behavior can be understood from Fig. 1. Taking the conduction subbands for example, for a given energy $E>0$, the more accurate band structure (the dashed lines in Fig. 1) yields two propagating bulk solutions $\pm k_1$ in the InGaAs layer, while the $\mathbf{k}\cdot\mathbf{p}$ band structure leads to four propagating bulk solutions $\pm k_2$ ($k_2\approx k_1$) and $\pm k_3$. The additional spurious degenerate states $\pm k_3$ on the spurious region of the conduction band ($|k_z|>k_c$) lead to fast oscillating spurious superlattice states. When the cutoff wave vector k_0 lies in the monotonic region of the conduction band $k_0\leqslant k_c$ [i.e., $N\leqslant 5$, as done in Fig. 2(a)], the fast oscillating spurious solutions are automatically excluded. For N=8 (N=10), spurious solutions appear at energies higher than 0.8 (0.4) eV, because only the high energy part $E\gtrsim 0.8$ eV ($E\gtrsim 0.4$ eV) of the spurious region is included within $k_0(=2N\pi/L)$. For N=20, the spurious region in the forbidden gap and in the valence bands is included, leading to the appearance of spurious solutions in these energy regions [see Fig. 2(d)]. Comparison between the results obtained with N=5 and those obtained following Ref. 8 shows that the differences for the lowest three conduction and valence subbands are smaller than 1.5 meV.

As a result, the first approach to remove spurious solutions is to choose a cutoff wave vector k_0 in the monotonically increasing region of the conduction band ($k_0\leqslant k_c$, cf. Fig. 1). Actually, as one of the advantages of the envelope function approximation, accurate results can be obtained by using a small number of plane waves.[17,18] From Fig. 1, we see that the error of the eight-band model increases with increasing energy. Especially for energies above $\sim$1.2 eV, wave vector components around the X_6 point of the more accurate band structure (obtained from the empirical pseudopotential method) should enter the envelope functions. This behavior cannot be reproduced by the eight-band model.

The second approach to eliminate spurious oscillatory solutions is to modify the Hamiltonian to produce monotonic bulk bands. Different approaches have been proposed along this line.[7–9] In Ref. 9, Kolokolov *et al.* introduced additional k^2 terms into the Hamiltonian and argued that introducing higher order terms $k^3,k^4,\ldots$ can reduce the error of the results. However, this has not been demonstrated due to the appearance of higher order derivatives in the numerical calculation. Using the finite plane-wave expansion, however, we are able to introduce arbitrary functions of the wave vector into the Hamiltonian without any complications. Then we gain some freedom to restore the monotonic bulk bands and, consequently, to compare the difference between the various approaches.

First, we introduce higher order terms of the wave vector k into the diagonal elements of the Hamiltonian to restore the monotonic behavior. For simplicity, we use the custom units defined by $e=\hbar=m_0=B_0=1$ (B_0=10 T) in the rest of this paper. Three types of functions (i) $f_1(\mathbf{k})=0.015|k_z^3|$, (ii) $f_2(\mathbf{k})=0.0004k_z^4$, and (iii) $f_3(\mathbf{k})=\theta(|k_z|-k_0)A_c(\mathrm{InGaAs})(k_0^2-k_z^2)$ ($k_0=10\pi/L$) are introduced into the conduction band elements H_{11} and H_{22}, respectively. The modified bulk band structures and the resulting superlattice subbands are shown in Fig. 3, where we also show the results obtained by (iv) following the proposal in Ref. 8 for comparison. It can be seen that although higher order terms $k^3,k^4,\ldots$ help to produce monotonic conduction bands for bulk InGaAs, they also lead to nonmonotonic light-hole bands for bulk InP. From Figs. 3(c) and 3(d), we see that the different modifications produce very close superlattice subbands, due to the close behaviors of the modified bulk bands at small wave vectors. The results from (i)–(iii) differ very small from (iv) for the lowest three subbands. For the conduction subbands, the difference is smaller than 3 meV (2 meV) for (i) [(ii) and (iii)]. For the valence subbands, the difference is less than 0.2 meV

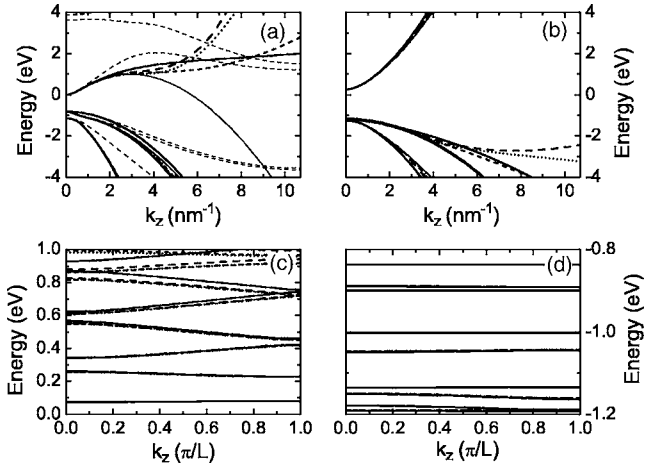

FIG. 4. Band structures of bulk (a) InGaAs and (b) InP as functions of k_z at $\mathbf{k}_\parallel=0$. The thin solid (thin dashed) lines are for the original $\mathbf{k}\cdot\mathbf{p}$ model (empirical pseudopotential method). (c) and (d) show the resulting superlattice subbands at $\mathbf{k}_\parallel=0$. In all panels, the solid, dashed, short-dashed, and dotted lines are for the modified models (i)–(iv), respectively. The cutoff number is taken as $N=15$.

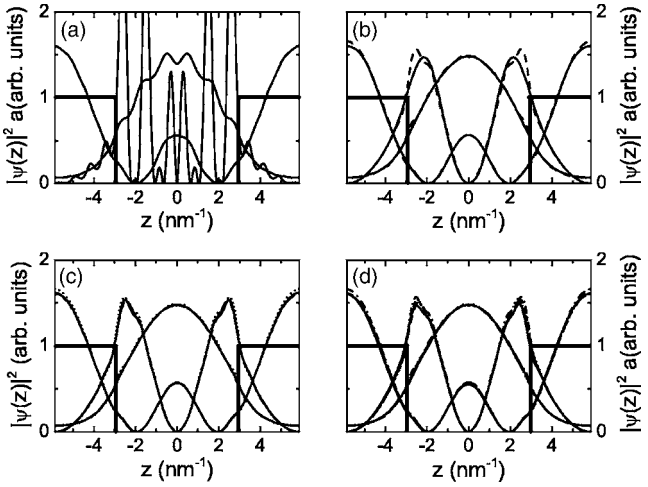

FIG. 5. Envelope functions of the lowest three conduction subbands at $\mathbf{k}_\parallel=0$. (a) and (b) show the solutions to the original Hamiltonian obtained with $N=15$ and $N=5$, respectively. (c) shows the results obtained by introducing additional terms into the diagonal elements of the Hamiltonian, (i) (solid lines), (ii) (dashed lines), and (iii) (short-dashed lines), as described in the text. (d) shows the results obtained by introducing additional terms into the off-diagonal elements of the Hamiltonian, (i) (solid lines), (ii) (dashed lines), (iii) (short-dashed lines), and (iv) (dotted lines), as described in the text. The results from Ref. 8 are also shown in panel (b) (dashed lines), (c) (dotted lines), and (d) (dash-dotted lines) for comparison. The cutoff number is taken as $N=15$ for (c) and (d).

for the first and third lowest subbands (which are of heavy-hole character), while it is less than 1 meV for the second lowest subbands (which is of light-hole character). The difference between the heavy-hole bands is significantly smaller, due to the vanishing electron-heavy hole coupling at $\mathbf{k}_\parallel=0$. The energy difference increases for higher excited states ($E\sim 1$ eV) due to the increasing difference between the modified bulk band structures [see Fig. 3(a) and Fig. 3(b)]. Note, however, that the envelope function approximation itself is invalid at such high energies (cf. Fig. 1).

Next, we explore the possibility to introduce higher order terms of k into the off-diagonal elements of the Hamiltonian. We choose to enhance the electron-light hole coupling by modifying the Kane parameter P in the terms $H_{14}=\sqrt{2/3}Pk_z$ and $H_{25}=i\sqrt{2/3}Pk_z$: (i) $P\rightarrow P+2.1ik_z$, (ii) $P\rightarrow P+0.05ik_z^2$, (iii) $P\rightarrow P+\theta(|k_z|-k_0)2.8i(|k_z|-k_0)$, and (iv) $P\rightarrow P+\theta(|k_z|-k_0)5.5i(|k_z|-k_0)^2/k_z$, where $k_0=8\pi/L$ (cf. Fig. 1). From Figs. 4(a) and 4(b), we see that the modified conduction bands of InGaAs are monotonic for (i)–(iv). However, introducing higher order terms k^3, k^4 [e.g., method (ii)] could lead to nonmonotonic light-hole bands for bulk InP [see the dashed lines in Fig. 4(b)]. The difference between the results from the different modified Hamiltonians is very small for low-lying subbands, and it increases with increasing energy. Specifically, those obtained from (i) (see the solid lines) are the highest, while those from (iii) and (iv) are the lowest, due to the same behavior of the modified bulk bands [see Fig. 4(a)]. However, as discussed previously, the envelope function approximation becomes invalid in this regime. We have compared the above results with those from Ref. 8. The difference for the lowest three conduction subbands is smaller than 2 meV. For the lowest light-hole (heavy-hole) subbands, the difference is less than 1.6 meV (0.002 meV). Again, we notice that the difference between heavy-hole bands is significantly smaller, because of the vanishing electron-heavy hole coupling strength at $\mathbf{k}_\parallel=0$.

From the above comparisons, we see that the typical difference among the results from the various modified Hamiltonians is several meV. Taking into account the difference (<1.5 meV) between the results from the wave vector cutoff method and those from Ref. 8, we see that the wave vector cutoff method could give an accurate enough description of the final results.

Now we turn to the envelope functions produced by the above various methods as shown in Fig. 5. First, we see that the lowest two subbands of the original Hamiltonian are strongly mixed with spurious solutions, while those obtained from the wave vector cutoff method [Fig. 5(b)] and other modified Hamiltonians show correct behaviors. Second, Fig. 5(b) shows that the envelope functions obtained from the wave vector cutoff method and those from Ref. 8 differ appreciably only near the interfaces. This is related to the comment in Ref. 8 that, discarding the large wave vector components, may contradict the usual interface conditions for the envelope functions. Actually, the envelope functions obtained from the wave vector cutoff method do not show rapid variation across the interfaces, since it does not have large wave vector components. In our opinion, these large wave vector components are caused by the steplike boundary conditions at the interfaces, which are, in fact, approximations to the true continuous boundary condition at the interfaces.[2] Further, the envelope function Hamiltonian is invalid at large wave vectors (e.g., outside the first Brillouin zone). As a result, reproducing such discontinuity by including the large wave vector components would not necessarily increase the accuracy of the final results. In principle, the cutoff wave vector for any envelope function Hamiltonian should not fall

outside the first Brillouin zone, where the envelope function Hamiltonian has become invalid. Third, we can see from Figs. 5(c) and 5(d) that the various modified Hamiltonians yield very similar, nonspurious envelope functions. Finally, it is worth noting that the accuracy of the various methods (relative to the true solutions) depends on the specific true band structures of the various materials. Better reproducing the small wave vector behavior of the original $\mathbf{k}\cdot\mathbf{p}$ bulk band structure would not necessarily lead to more accurate results. For example, in Fig. 2(a), the deviation of the original $\mathbf{k}\cdot\mathbf{p}$ band structure from the true band structure is the most serious compared with other modified ones. Reproducing the original band structure exactly may decrease (not increase) the accuracy of the final results.

At this point, it would be beneficial to discuss the choice of the different approaches to avoid spurious solutions. The proposal in Ref. 8 does not need to modify the structure of the original Hamiltonian, while other modifications are based on mathematical tricks which do not arise from the $\mathbf{k}\cdot\mathbf{p}$ theory. However, modifying the Kane parameter P as suggested in Ref. 8 would inevitably modify the effective mass of the spin-orbit split-off band. Therefore, it is better to use the wave vector cutoff method or the method of introducing additional terms when we are concerned with the states derived from the spin-orbit split-off bands. For other cases, it is better to use the approach in Ref. 8 or the wave vector cutoff method, since they do not need to modify the structure of the original Hamiltonian.

In summary, we have investigated the origin of spurious oscillatory solutions in the eight-band envelope function model. We found that it arises from the additional spurious degeneracies caused by the unphysical bowing of the bulk conduction bands. Two categories of approaches to eliminate spurious solutions have been proposed. One is the wave vector cutoff method, which does not require to modify the original Hamiltonian. Based on a finite plane-wave expansion method, we have demonstrated the origin and elimination of spurious oscillatory solutions in a transparent way. The other is to modify the Hamiltonian to produce monotonic bulk bands. The existing proposals are extended such that we gain some freedom in modifying the Hamiltonian. The energies and envelope functions obtained from the various approaches have been compared, yielding energy differences of the order of several meV. It suggests that the wave vector cutoff method can give an accurate enough description to the final results.

This work was supported by the NSFC Grant No. 60376016, 863 Project No. 2002AA31, and the special fund for Major State Basic Research Project No. G001CB3095 of China.

*Author to whom correspondence should be addressed. Electronic address: kchang@red.semi.ac.cn

[1] E. O. Kane, in *Handbook of Semiconductors*, edited by W. Paul (North-Holland, Amsterdam, 1982).
[2] M. G. Burt, J. Phys.: Condens. Matter **4**, 6651 (1992).
[3] S. R. White and L. J. Sham, Phys. Rev. Lett. **47**, 879 (1981).
[4] D. L. Smith and C. Mailhiot, Phys. Rev. B **33**, 8345 (1986).
[5] F. Szmulowicz, Phys. Rev. B **54**, 11539 (1996).
[6] M. F. H. Schuurmans and G. W. 't Hooft, Phys. Rev. B **31**, 8041 (1985).
[7] R. Eppenga, M. F. H. Schuurmans, and S. Colak, Phys. Rev. B **36**, 1554 (1987).
[8] B. A. Foreman, Phys. Rev. B **56**, R12748 (1997).
[9] K. I. Kolokolov, J. Li, and C. Z. Ning, Phys. Rev. B **68**, 161308(R) (2003).
[10] R. Winkler and U. Rössler, Phys. Rev. B **48**, 8918 (1993).
[11] M. J. Godfrey and A. M. Malik, Phys. Rev. B **53**, 16504 (1996).
[12] W. Trzeciakowski, Phys. Rev. B **38**, 12493 (1988).
[13] A. T. Meney, B. Gonul, and E. P. O'Reilly, Phys. Rev. B **50**, 10893 (1994).
[14] Lin-Wang Wang, Phys. Rev. B **61**, 7241 (2000).
[15] I. Vurgaftmana, J. R. Meyer, and L. R. Ram-Mohan, J. Appl. Phys. **89**, 5815 (2001).
[16] K. Kim, P. R. C. Kent, A. Zunger, and C. B. Geller, Phys. Rev. B **66**, 045208 (2002).
[17] J. B. Xia, Phys. Rev. B **39**, 3310 (1989).
[18] L. W. Wang, A. Franceschetti, and A. Zunger, Phys. Rev. Lett. **78**, 2819 (1997); L. W. Wang and A. Zunger, Phys. Rev. B **59**, 15806 (1999).